

# Gate-voltage control of spin interactions between electrons and nuclei in a semiconductor

J. H. Smet\*, R. A. Deutschmann†, F. Ertl‡, W. Wegscheider†§, G. Abstreiter† & K. von Klitzing\*

\* Max-Planck-Institut für Festkörperforschung, D-70569 Stuttgart, Germany

† Walter Schottky Institut, Technische Universität München, D-85748 Garching, Germany

§ Institut für Experimentelle und Angewandte Physik, Universität Regensburg, D-93040 Regensburg, Germany

**Semiconductors are ubiquitous in device electronics, because their charge distributions can be conveniently manipulated with voltages to perform logic operations. Achieving a similar level of control over the spin degrees of freedom, either from electrons or nuclei, could provide intriguing prospects for both information processing and the study of fundamental solid-state physics issues. Here we report procedures that carry out the controlled transfer of spin angular momentum between electrons—confined to two dimensions and subjected to a perpendicular magnetic field—and the nuclei of the host semiconductor, using gate voltages only. We show that the spin transfer rate can be enhanced near a ferromagnetic ground state of the electron system, and that the induced nuclear spin polarization can be subsequently stored and ‘read out’. These techniques can also be combined into a spectroscopic tool to detect the low-energy collective excitations in the electron system that promote the spin transfer. The existence of such excitations is contingent on appropriate electron–electron correlations, and these can be tuned by changing, for example, the electron density via a gate voltage.**

Discussions of future information-processing technologies often assign a prominent role to the spin degree of freedom in addition to (or instead of) the charge degree of freedom<sup>1</sup>, which is exploited in today’s mainstream electronics. In the short term, this ‘spintronics’ may deliver products with enhanced functionality or improved performance, such as high-speed, high-density non-volatile random access memories: whereas on a much longer timescale, contributions to the very challenging realm of quantum computation<sup>2,3</sup> have been anticipated. Quantum computation attempts to benefit from correlations and dissipationless transformations of coupled quantum-mechanical systems. The main incentive is a certain degree of parallelism that computational schemes based on such principles bring with them. For example, such schemes offer algorithms for prime factorization<sup>4</sup> and for exhaustive search<sup>5</sup>; unlike any apparatus based on classical physics, a quantum computer should be able to solve these problems in polynomial time—provided that it can be implemented in a real machine, as energy dissipation is a fundamental source of concern. There has been a wide variety of proposals for practical implementations of rudimentary logic gates in which quantum memory registers—based on any of the abundant two-level systems in physics, like spin-1/2 electrons and nuclei—can be externally manipulated. These proposals range from trap configurations in atom or ion physics<sup>6</sup>, to techniques of nuclear magnetic resonance spectroscopy<sup>7,8</sup> as used in organic chemistry, to a very bold all-electronic approach for nuclear spin solid-state devices<sup>9</sup> that would marry the merits of electronics fabrication technology with the virtues of quantum computation<sup>10</sup>.

Many of the ideas produced by workers in the spintronics and quantum computing communities may be deemed far out of reach. But they have sparked efforts to develop new ways to accomplish the more fundamental task of controlling and measuring the nuclear spin polarization in solid-state devices, in view of the dearth of existing techniques for locally manipulating nuclear spins. Particularly appealing is the use of mobile objects, like conduction electrons in semiconductors, as mediators to both probe and modify nuclear spins. Gating and optical techniques are able to tailor precisely the population and energy distribution of such electrons, especially

when they are constrained to move in two dimensions—as in quantum wells or field-effect transistors—or even fewer dimensions. The creation of non-equilibrium populations of spin-polarized electrons using coherent polarized light pulses or gating techniques have, for example, already enabled dynamical control of nuclear spins or the electronic generation of net nuclear spin polarization<sup>11–13</sup>. Progress in this area will rely on experiments specifically geared towards expanding limited knowledge of controlled spin interactions and the microscopic interaction processes that take place between spin systems in such low-dimensional structures. It constitutes the main motivation for the work presented here.

The electrons and nuclear spins in a semiconductor are coupled through the hyperfine interaction. For electrons in the conduction band described by *s*-type Bloch functions the contact hyperfine Fermi interaction prevails<sup>14</sup>. It allows the simultaneous reversal of a nuclear and an electronic spin while preserving total spin angular momentum and energy. This flip-flop scattering mechanism may either serve as a relaxation channel to equilibrate the nuclear spin degrees of freedom with the lattice, or as a means of dynamically polarizing and cooling them if the electronic spin system is first brought out of equilibrium. However, in a two-dimensional electron system<sup>15</sup> (2DES) based on GaAs and subjected to a strong perpendicular magnetic field  $B_{\perp}$ , nuclear spins precess at frequencies some three orders of magnitude below that of the electronic Zeeman gap—which is the energy required to flip a single electronic spin. This large discrepancy normally impedes efficient spin transfer in this regime, so that the nuclear and electronic systems are well isolated. But this barrier for spin transfer can be overcome by taking into account Coulomb correlations inherent in the 2DES: at specific electron densities, which can be controlled by a gate voltage, these correlations contrive low-energy or gapless collective excitations that better match the nuclear spin energy levels, so that efficient channels to convey spin angular momentum between both spin systems can be opened up at these densities.

Here we provide evidence that by varying the carrier density  $n_{2D}$  of the 2DES at a fixed field  $B_{\perp}$  through a gate voltage, the state of the nuclear spin system can indeed be manipulated, read out and

stored. Spatial variations in the nuclear polarization are generated when the 2DES condenses in a ground state with ferromagnetic order<sup>16,17</sup> and a rapid thermal equilibration is achieved at carrier densities where gapless spin wave modes<sup>18</sup> (associated with the in-plane magnetic order of finite-size skyrmions, complex spin textural defects<sup>19–21</sup>) are believed to exist. Depletion of the 2DES interrupts flip-flop scattering, and the nuclear spin configuration is stored. Dwelling at other electron densities, where the energy conservation rule for flip-flop scattering can not be fulfilled, also quenches the hyperfine interaction and the nuclear spin orientation is maintained. The degree of nuclear spin polarization acts back on the electronic system and relocates the ferromagnetic ordered ground

state to higher fields, so that its position reveals the degree of nuclear spin polarization.

### The Ising ferromagnetic state

The quantization of the electron cyclotron motion in a field  $B_{\perp}$  and the Zeeman coupling of  $B_{\perp}$  to the electron spin degree of freedom discretizes the energy spectrum of a 2DES into a ladder of spin-split Landau levels. Each level is classified by its orbital radius and spin quantum number, and possesses a macroscopic degeneracy per unit area  $d = B_{\perp}/\Phi_0$  where  $\Phi_0$  is the flux quantum<sup>15</sup>. The filling factor  $\nu = n_{2D}/d$  denotes the number of filled Landau levels. A similar effect occurs by virtue of the Coulomb interaction when all electrons reside in the lowest Landau level. When it is half filled, composite fermions<sup>22</sup>—quasiparticles assembled from one electron and two flux quanta—make up a metallic state and a fan of composite-fermion Landau levels develops away from filling factor  $\nu = 1/2$ . If an integer number  $p$  of electron Landau levels is filled, the 2DES condenses in an integer quantum Hall state<sup>23</sup> with its vanishing conductance along the current direction and quantized Hall conductance. Analogously, if an integer number  $q$  of composite-fermion Landau levels is occupied (equivalent to fractional fillings of the lowest electron Landau level of the form  $\nu = q/(2q \pm 1)$ ), the fractional quantum Hall effect<sup>24,25</sup> ensues.

When two electron or composite-fermion Landau levels simultaneously approach the chemical potential, correlations frequently force the 2DES to order in a ferromagnetic ground state<sup>16,17,26–29</sup> similar to those of conventional low-dimensional ferromagnets. If the Landau levels have opposite spin quantum numbers and different cyclotron energies, the exchange energy cost for spin misalignment forces those particles that are to be distributed among the nearly coincident Landau levels to take on identical spin orientation, either along or opposite to the Zeeman field. It induces an Ising-like ferromagnetic phase transition with easy-axis anisotropy between quantum Hall states with distinct spin configurations as one Landau level overtakes the other. It is heralded in the transport properties of the 2DES by the disappearance of the quantum Hall effect. This first-order phase transition is accompanied by hysteresis and extra dissipation due to the domain morphology, which acts as an additional source of backscattering for current-carrying quasiparticles. An example is shown in Fig. 1 for the spin-unpolarized and fully spin-polarized  $\nu = 2/3$  fractional quantum Hall states when two composite-fermion Landau levels are completely occupied, and the spin-down state of the lowest level and the spin-up state of the second level are brought close to degeneracy (this and all other experiments were performed at the base temperature of a 20 mK dilution refrigerator). The quantized kinetic energy of composite fermions originates from the Coulomb interaction energy  $E_C$ , and grows with  $\sqrt{n_{2D}}$  or equivalently  $\sqrt{B_{\perp}}$  at fixed filling, whereas the Zeeman splitting  $E_Z$  goes linearly. This phase transition can thus be conveniently driven by tuning the carrier density and occurs at a critical ratio of both energy scales.

In the presence of spin orientation, the hyperfine interaction also causes nuclear ( $B_N$ ) and electronic ( $B_e$ ) magnetic fields that act respectively on the electronic and nuclear spins, as manifested for example by Overhauser and Knight shifts in their energy spectrum<sup>14</sup>. The hyperfine effective nuclear field  $B_N$  only alters the electronic Zeeman energy, so that  $E_Z/E_C \propto (B_{\perp} + B_N)/B_{\perp}^{1/2}$ . From the external field  $B_{\perp}$  or density for which  $E_Z/E_C$  exceeds the critical value that triggers the Ising ferromagnetic phase transition, the degree of nuclear spin orientation  $B_N$  can be extracted. A gradual polarization of the nuclear spin system as time progresses should leave a ‘fingerprint’ in the source–drain resistance  $R_{SD}$  as the phase transition is relocated, provided that the fixed working point ( $n_{2D}, \nu \approx 2/3$ ) at which  $R_{SD}$  is monitored is chosen skilfully.

### Flipping of nuclear spins

At the transition, the sample is unable to reach instantaneously its

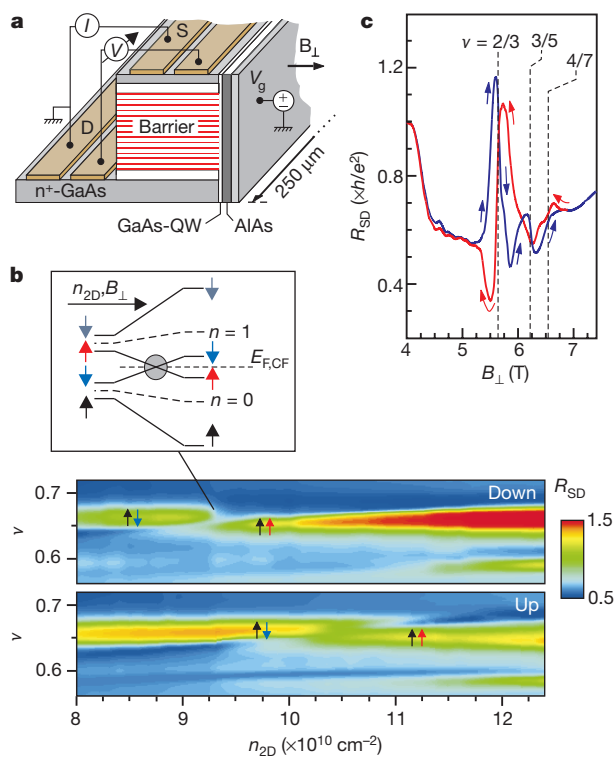


**Figure 1** Ferromagnetic phase transition with easy-axis anisotropy between the spin-unpolarized and fully spin-polarized  $2/3$  fractional quantum Hall states. **a**, The device is a field-effect transistor on the cleaved edge of a GaAs (001) substrate with a channel length of  $3 \mu\text{m}$  and width of approximately  $250 \mu\text{m}$ . In a first growth sequence along the (001) direction, a superlattice barrier is sandwiched between two conducting  $n^+$ -GaAs layers that form the source (S) and drain (D) contacts. Subsequently, the sample is cleaved *in situ* and a thin GaAs layer (GaAs-QW) is deposited on the freshly exposed (110) surface. It will host the 2DES. It is capped by an AlAs barrier and an  $n^+$ -GaAs layer that serves as the gate. A positive gate voltage  $V_g$  with respect to source and drain induces the 2DES electrostatically at the GaAs/AlAs heterointerface. For this geometry, a plateau appears in the source–drain resistance  $R_{SD}$  when the 2DES condenses in a quantum Hall state (or a maximum if it is not fully developed)<sup>17</sup>. In between two such states, the non-zero source–drain conductivity partly short-circuits the Hall voltage and therefore  $R_{SD}$  drops and displays a minimum. **b**, Two-dimensional graphs of  $R_{SD}$  (colour) versus carrier density  $n_{2D}$  and filling factor  $\nu$  near  $\nu = 2/3$  in units of  $h/e^2$ . The data acquisition is performed during downward (top) and upward (bottom) sweeps of the magnetic field. The hysteretic phase transition is signalled by the disappearance of the  $\nu = 2/3$  quantum Hall maximum. Inset: at the coincidence of the composite-fermion spin-up Landau level with orbital index  $n = 1$  and the composite-fermion spin-down Landau level with index  $n = 0$ , the unpolarized  $2/3$  fractional quantum Hall state (black and blue arrows indicate the spin orientation of the participating filled levels) vanishes and the fully spin-polarized  $2/3$  fractional quantum Hall state (black and red arrows) emerges. ( $E_{F,CF}$  is the Fermi level.) **c**, Example of hysteresis in an  $R_{SD}$  trace when reversing the magnetic field sweep direction.

stationary or thermodynamic equilibrium state. Figure 2 illustrates the delayed response of the resistance after a magnetic field sweep or change in gate voltage took place. We believe that the sample steadily approaches equilibrium with the aid of the hyperfine interaction, and that the initial time dependence of the resistance mainly reflects a gradual change in the nuclear spin polarization. The non-equilibrium character may originate from either the electronic system itself or the nuclear lattice. In the ferromagnetic state, energy barriers control the dynamics of domain walls, and the electronic system may be trapped in a metastable state due to a local free energy minimum. The growth of domains requires spin flips that can be mediated by the underlying nuclear lattice. Because the degree of electron spin polarization can be drastically modified with filling factor and thus magnetic field or gate voltage, the nuclear spin system may have been brought out of equilibrium by sweeping the external field or carrier density. The involvement of nuclear spins has been previously inferred from resistively detected NMR in this regime<sup>17,30</sup>. Other evidence is depicted in Fig. 2. During removal of all charge carriers from the 2DES for a short interval, the resistance change halts<sup>31</sup>. Subsequently it continues as if depletion had not taken place. Only the nuclear spins can be invoked as the storage medium for the domain configuration in the absence of charge carriers. We will now substantiate the above claims—but we will first illustrate how the nuclear spin system may be returned to a well-defined, reproducible initial state ('reset') irrespective of the previous history of the sample, an essential ability for a systematic investigation of these phenomena.

### 'Reset' procedure for the nuclei

At Landau level filling factor  $\nu = 1$ , quantum Hall systems exhibit Heisenberg-like isotropic itinerant ferromagnetic order in their ground state<sup>20</sup>. The Coulomb exchange energy penalty for reversed spins exactly complete spin alignment of the free electrons, even in the limit of vanishing Zeeman coupling strength. Furthermore, at sufficiently weak Zeeman coupling it turns finite-size skyrmions or anti-skyrmions<sup>20,32</sup> (instead of single spin flip excitations) into the lowest-energy charged excitations of this incompressible ground state. These circularly symmetric spin textural defects have their spins aligned with the Zeeman field at the perimeter, gradually reversed towards their centre to keep the exchange cost to a minimum, and possess non-zero in-plane spin components with a vortex-like configuration at intermediate distances. They accommodate precisely one extra unit of charge, and yet flip numerous spins depending on their spatial extent. This spatial extent is set by

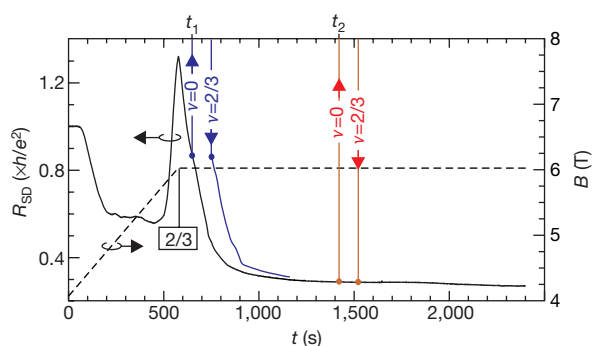


**Figure 2** Time dependence of  $R_{SD}$  near filling factor  $\nu = 2/3$  after a field sweep. The magnetic field sweep starts from  $\nu = 1$  and is interrupted at  $\nu = 2/3$ .  $R_{SD}$  continues to change. The experiment is then repeated, but at times  $t_1$  (blue curve) and  $t_2$  (red curve) all charge carriers are removed for 90 s by reducing the gate voltage to zero. When the original carrier density is restored, the resistance continues its descent from nearly the same value as if the time interval during which the sample was fully depleted never took place.

the competition between the Zeeman coupling, which attempts to reduce the number of flipped spins by covering a small area, and the Coulomb interaction, which favours a uniform charge distribution across a large area. At exactly  $\nu = 1$ , skyrmions freeze out and disappear at low temperatures. However, when moving away from filling factor  $\nu = 1$ , for each unit of charge added or subtracted from the 2DES a skyrmion or anti-skyrmion is generated. At a finite density of skyrmions, it has been proposed that they crystallize in the sufficiently dilute limit<sup>33</sup>. The classical energy of an isolated skyrmion is invariant for translations in real space and uniform rotations in spin space about the axis defined by the Zeeman field. In a crystalline configuration the spin rotational and translational symmetries are broken, and these degrees of freedom give rise to gapless low-energy collective excitations in the theory<sup>18</sup>. Even if the crystal melts at higher skyrmion densities, these modes presumably remain present in an overdamped form. The gapless spin wave Goldstone mode then provides an efficient channel for flip-flop scattering, as the energy conservation criterion for the Fermi contact interaction can be met. This mode has been invoked as one possible explanation to account for both the rapid nuclear spin relaxation rate in optically pumped NMR experiments<sup>21,34</sup> and the enormous enhancement of the specific heat<sup>35</sup> due to the entropy of the nuclei near (but away from) exact filling  $\nu = 1$ .

Here we exploit these previously reported short nuclear spin relaxation times  $T_1$  in the skyrmion regime to bring the nuclear spin

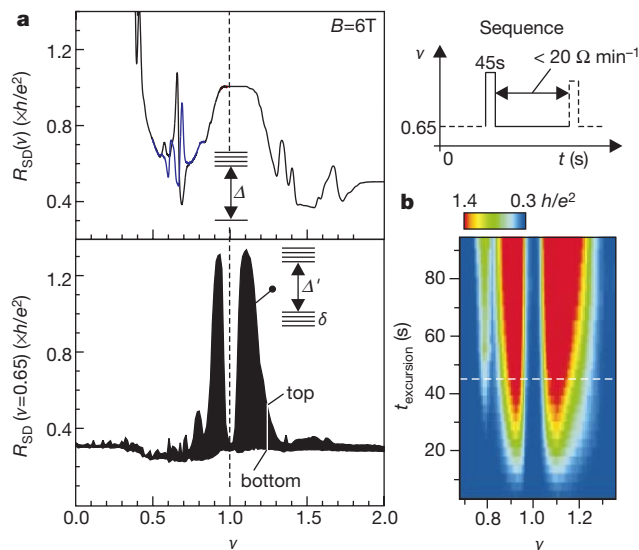


**Figure 3** Time dependence of  $R_{SD}$  after a short excursion from filling factor  $\nu = 0.65$  to filling factor  $\nu$  at fixed magnetic field. **a**, Top panel:  $R_{SD}$  as a function of  $\nu$  obtained by sweeping the carrier density down (blue curve) or up (black curve) at fixed magnetic field. Bottom panel: the measurement sequence executed to obtain the data in this panel is depicted in the inset on the right.  $R_{SD}$  is left to relax at  $\nu = 0.65$  until  $dR_{SD}/dt < 20 \Omega \text{ min}^{-1}$  (dashed line). Then, a new measurement sequence starts (solid line). First, a  $t_{\text{excursion}} = 45 \text{ s}$  excursion to filling factor  $\nu$  is performed. The resistance upon return to  $\nu = 0.65$  is recorded (envelope top) and its subsequent time dependence is plotted along the vertical axis until  $dR_{SD}/dt < 20 \Omega \text{ min}^{-1}$  (envelope bottom). The same procedure is then repeated for a different filling factor (dashed line on the right of the insert describing the measurement sequence). The data are also featureless from  $\nu = 2$  up to the maximum reachable filling factor of 3.3 (limited by the gate leakage current, data not shown). The energy diagrams indicate schematically that only near (but away from)  $\nu = 1$  low-energy collective excitation modes ( $\delta$ ) exist, compatible with the energy spectrum of the nuclei.  $\Delta'$  and  $\Delta$  are the energy required to create a single finite-size skyrmion. At exact filling factor  $\nu = 1$ , the large gap  $\Delta$  prevents flip-flop scattering. **b**, Same as before, but with  $t_{\text{excursion}}$  as an additional parameter.  $R_{SD}$  at  $t = 0 \text{ s}$  upon return is plotted (red corresponds to high values, blue to low values). Dashed white line corresponds to the envelope top in **a** for  $t_{\text{excursion}} = 45 \text{ s}$ .

system into thermal equilibrium with the GaAs lattice for a specific filling factor near  $\nu = 1$ . The history-dependent nuclear spin polarization acquired near the  $\nu = 2/3$  ferromagnetic phase transition is erased. Figure 3a illustrates the recovery of the high values of source–drain resistance  $R_{SD}$  near the  $\nu = 2/3$  ground-state spin transition after a short excursion ( $t_{\text{excursion}} = 45$  s) of the sample at fixed magnetic field to filling factors  $\nu$  close to, but distinct from,  $\nu = 1$ . The difference in  $R_{SD}$  at  $\nu = 0.65$ ,  $\Delta R_{SD}$ , between its value at  $t = 0$  directly upon return to  $\nu = 0.65$  from filling factor  $\nu$  and its value at large  $t$  (defined as  $dR_{SD}/dt < 20 \Omega \text{ min}^{-1}$ ) is a measure of the nuclear spin–lattice relaxation time  $T_1$ , and provides indirect information on the available electronic many-particle energy states at filling factor  $\nu$ . The data exhibit maxima near  $\nu = 0.92$  and 1.1, and reproduce qualitatively the behaviour of  $T_1$  obtained from optically pumped NMR experiments<sup>21,34</sup>. At  $\nu = 1$ , in the absence of skyrmions and the associated low-energy collective modes, the nuclear spin polarization state is left unaltered and stored. By including  $t_{\text{excursion}}$  as an additional parameter in Fig. 3b, values of  $T_1$  of around 20 s at  $\nu = 0.9$  are estimated from the saturation of  $\Delta R_{SD}(t_{\text{excursion}})$ , in

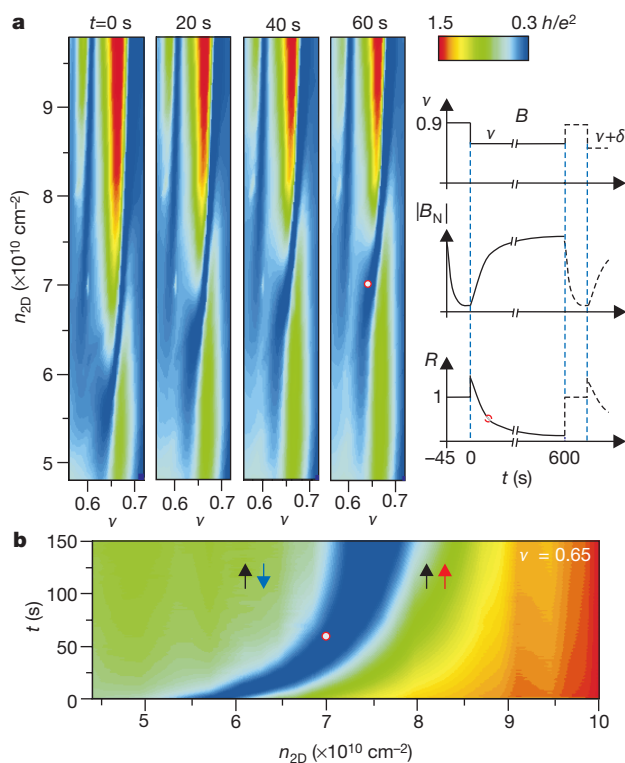


**Figure 4** Time progression of the ferromagnetic phase transition. The time dependence of  $R_{SD}$  is acquired for closely spaced coordinates in the  $(\nu, n_{2D})$ -plane by following the measurement sequence depicted on the right. Before recording the time dependence at a certain  $(\nu, n_{2D})$ -pair, the filling factor is set to  $\nu = 0.9$  for 45 s. The nuclear spin system of the host GaAs crystal is allowed to relax to its thermal equilibrium state for this filling factor due to the enhanced flip-flop scattering rate under these conditions. It ensures a well-defined, history-independent starting point. After recording  $R_{SD}$  for 600 s, either the magnetic field or gate voltage is swept to the next  $(\nu, n_{2D})$ -pair and the above procedure is repeated (dashed line in the inset plotting the measurement sequence). Several sections through the three-dimensional parameter space  $(t, \nu, n_{2D})$  are displayed. The resistance values are colour coded (red, high resistance values; blue, small resistance values). **a**, From left to right:  $R_{SD}(\nu, n_{2D})$  at time  $t = 0, 20, 40, 60$  s. **b**,  $R_{SD}(n_{2D}, t)$  at fixed filling factor  $\nu = 0.65$ . This graph and similar cuts through the data at nearby filling factors and extended to longer times  $t$  are an aid to selecting a suitable working point at which the source–drain resistance is monitored for the experiments plotted in Figs 3, 5–7. Working points meet the following criteria: monotonic behaviour and maximum swing of  $R_{SD}$  for the variation in  $B_N$  relevant to the experiments. The white dot with red border is the data point for  $(t = 60$  s,  $\nu = 0.65$ ,  $n_{2D} = 7 \times 10^{10} \text{ cm}^{-2}$ ).

agreement with ref. 34. Thus, staying for more than 40 s at  $\nu = 0.9$  apparently suffices to reset the nuclear spin lattice to a well-defined state and wipe out any previous history.

**Putting it all together**

This reset procedure is the key to the corroboration of our initial assertion that the time dependence of  $R_{SD}$  and the hysteretic behaviour at the ferromagnetic phase transition (Figs 1 and 2) mainly originate from a gradual polarization change of the nuclear

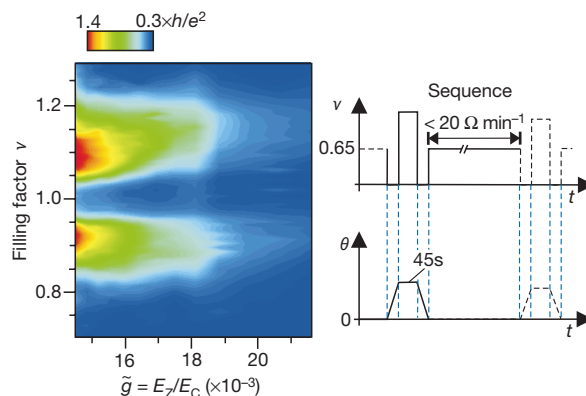


**Figure 5** The ratio  $E_Z/E_C$  can be changed by tilting the sample *in situ* with respect to the axis of the superconducting magnet. ( $E_C$  is the Coulomb interaction energy, and  $E_Z$  is the Zeeman splitting.) This is because the Coulomb interaction scales with the perpendicular component of the magnetic field only, whereas the Zeeman energy is determined by the total field. The magnet produces a fixed field of 6 T during the entire experiment. The nuclear spin relaxation rate near  $\nu = 1$  is investigated as in Fig. 3, but as a function of  $E_Z/E_C$  by executing the following measurement sequence:  $R_{SD}$  is left to relax at  $\nu = 0.65$  until  $dR_{SD}/dt < 20 \Omega \text{ min}^{-1}$ . Subsequently, all charge carriers are removed and the sample is rotated with a nearly frictionless mechanism from  $\theta = 0$  to  $\theta = \alpha$  within a time of 40 s, independent of the final angle set.  $\theta$  is defined as the angle between the magnetic field and the direction perpendicular to the 2DES. In the absence of charge carriers during rotation, the transfer of spin angular momentum is interrupted and the nuclear spin configuration is retained as proven in Fig. 2. The system is then left to relax for 45 s at a filling factor  $\nu$  near 1. The 2DES is depleted once more for 40 s. During this time, the sample is reoriented perpendicular to the field. The original filling factor  $\nu = 0.65$  is restored, and  $R_{SD}$  is acquired immediately afterwards.  $R_{SD}$  is allowed to relax, so that a new sequence at different  $\nu$  or angle can be started. The procedure ensures that  $E_Z/E_C$  is always the same at  $\nu = 0.65$ , so that only the influence of a variation in  $E_Z/E_C$  on the skyrmion physics near  $\nu = 1$  is tested. The skyrmion size gradually shrinks, and eventually the square lattice configuration becomes unstable and the spin wave Goldstone modes vanish according to theory<sup>18</sup>. The hyperfine interaction is quenched, and  $R_{SD}$  experiences essentially no change after the 45 s excursion to a filling factor near  $\nu = 1$ .

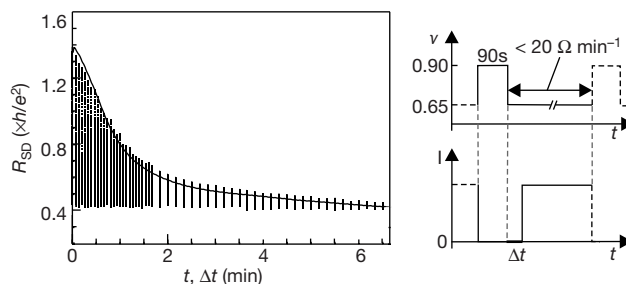


**Figure 6** Time behaviour of  $R_{SD}$  in the absence of current flow. Thick solid line;  $R_{SD}(t)$  at  $\nu = 0.65$  and  $B = 5.8$  T after equilibrating the nuclear spin system for 90 s at  $\nu = 0.9$ . Vertical lines; after an excursion of 90 s to  $\nu = 0.9$  to return to a well-defined state of the nuclear spin system, the current remains switched off for a time  $\Delta t$ . Subsequently, the resistance is recorded along the vertical axis at abscissa  $\Delta t$  until  $dR_{SD}/dt$  is smaller than  $20 \Omega \text{ min}^{-1}$ . The same procedure is then repeated for different values of  $\Delta t$ .

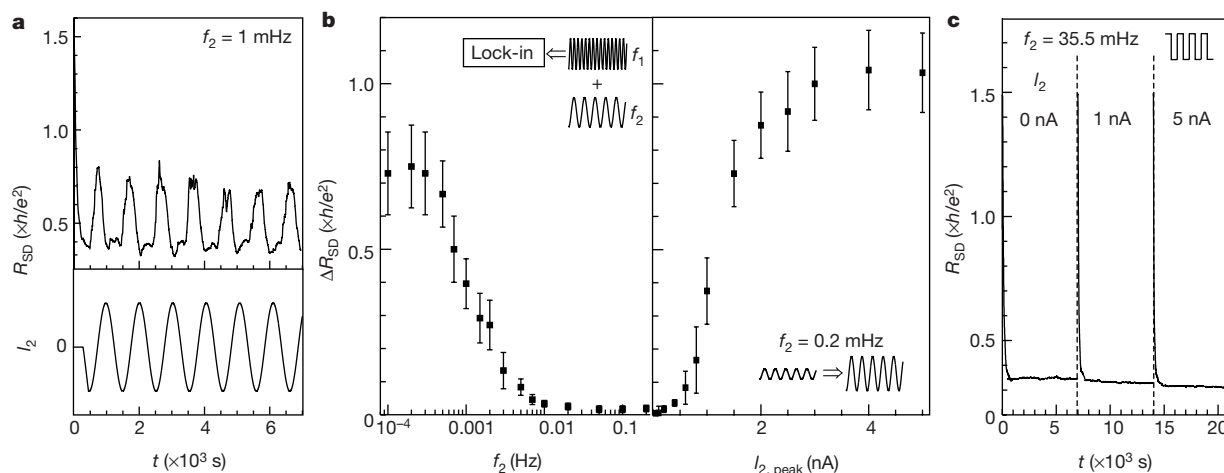


**Figure 7** Current-induced displacement of the ferromagnetic phase transition. The following operations are performed to study the influence of current flow. After equilibration of the nuclear spins at  $\nu = 0.9$  for 90 s,  $R_{SD}$  is monitored with time at  $\nu = 0.65$  in the presence of an alternating current with frequency  $f_1 = 5.36$  Hz and amplitude  $I_1 = 1$  nA. An alternating current with variable amplitude  $I_2$  and frequency  $f_2$ , outside the detection band of the lock-in amplifier utilized to record  $R_{SD}$ , is added after 500 s. During the first 500 s the initial rapid drop in  $R_{SD}$  took place, associated with the relocation of the phase transition to higher fields due to the change in the net nuclear spin polarization.  $R_{SD}$  is then measured for at least 6 periods of this extra alternating current component  $I_2$ .  $B_{\perp}$  is left fixed at all times (5.8 T). **a**,  $R_{SD}$  obtained in this fashion for  $f_2 = 1$  mHz and  $I_2 = 1.5$  nA.

$R_{SD}$  partially returns to its high value immediately after equilibration of the nuclear spin system at  $\nu = 0.9$ . This is reversible. Its low value is recovered when the sign of the current changes. This experiment suggests that current-driven dynamic nuclear spin polarization erases part of the net nuclear spin polarization when current flows in a particular direction. In the opposite direction the nuclear spin polarization is enhanced. **b**, Left panel: amplitude of the periodic change  $\Delta R_{SD}$  as a function of  $f_2$  at fixed  $I_2 = 1.5$  nA. Error bars indicate the spread in the observed change. Right panel:  $\Delta R_{SD}$  as a function of  $I_2$  for a fixed frequency  $f_2 = 0.2$  mHz. **c**, To verify that the additional dissipation due to  $I_2$  can be excluded as the origin of  $\Delta R_{SD}$ ,  $R_{SD}(t)$  is measured for a square wave with  $f_2 = 35.5$  Hz and  $I_2$  up to 5 nA.

spin lattice.  $R_{SD}$  is recorded in the three-dimensional parameter space ( $\nu, n_{2D}, t$ ) for  $\nu = 0.56 \dots 0.72, n_{2D} = 4.8 \times 10^{10} \dots 9.8 \times 10^{10} \text{ cm}^{-2}$  and  $t = 0 \dots 600$  s by repeatedly equilibrating the nuclear spin lattice at  $\nu = 0.9$  for any pair ( $\nu, n_{2D}$ ). Figure 4 depicts two-dimensional cross-sections through the data, collected in this fashion, either at a fixed time  $t = 0, 20, 40$  and  $60$  s (Fig. 4a) or a fixed filling factor  $\nu = 0.65$  (Fig. 4b). The ferromagnetic phase transition progressively shifts to larger carrier densities, or equivalently magnetic fields, as time passes. A time-dependent  $B_N(t)$  then provides a natural interpretation of the data, since the critical ratio  $E_Z/E_C \propto [B_{\perp} + B_N(t)]/B_{\perp}^{1/2}$ , at which the ferromagnetic phase transition due to the coincidence of two composite-fermion Landau levels occurs, is attained at a time-dependent external critical field. The relocation to higher  $B_{\perp}$  implies a depolarization of the electronic system and an upward polarization of the nuclear spins, inducing a  $\Delta B_N$  opposite to the external  $B_{\perp}$ . From the data at time  $t = 0$  (Fig. 4a) and  $t \gg 0$  (for example Fig. 1b, no equilibration of the nuclear spin lattice at  $\nu = 0.9$ ), we extract a change in the effective nuclear field of up to  $\Delta B_N \approx -0.8$  T on a timescale of a few minutes only. The hysteresis observed in Fig. 1b and c may thus in part be accounted for as originating from a different degree of nuclear spin orientation accumulated in the course of the complex path followed by field and gate voltage to map the resistance in the  $(n_{2D}, \nu)$ -plane.

This apparently efficient transfer of spin angular momentum to the nuclear lattice near  $\nu = 2/3$  strongly suggests the availability of low-energy collective electronic excitations specific to the ferromagnetic state. At present, we can only speculate on their microscopic nature, as ferromagnetism in the fractional quantum Hall regime has not so far been treated theoretically. These collective excitations are probably generated at and localized to the domain boundaries only, where they are presumably responsible for gradually reversing the spin in a Bloch wall between adjacent domains of distinct spin configurations. The procedures developed here may more generally be applied as a spectroscopy tool to unveil the absence or presence of gapless or low-energy collective modes. A

sophisticated example is depicted in Fig. 5. By selectively enhancing the Zeeman energy over the Coulomb energy scale through the addition of an in-plane magnetic field near  $\nu = 1$ , the skyrmions shrink in size and approach the single spin flip excitation limit. According to theory<sup>18</sup>, the square lattice configuration should become unstable and the spin wave Goldstone modes should vanish—apparently in agreement with this experiment.

### Irrelevance of external current flow

It is a common premise that dynamic nuclear spin polarization of this magnitude demands current flow, in view of the large discrepancy between the electron number and the number of nuclei involved. Contacts serve as source or sink of electronic spin in this open system. Yet current flow is not compulsory for the progressive relocation to higher carrier densities of the ground-state spin transition in Fig. 4. Figure 6 illustrates that, even in the absence of any source–drain current,  $R_{SD}$  evolves in time along nearly the same curve. A non-equilibrium in the electronic system—due to the domain morphology in the ferromagnetic state—and/or the nuclear spin system—as a result of different degrees of electron spin polarization and corresponding Knight shifts between  $\nu = 0.65$  and  $\nu = 0.9$ —is the suggested impetus for exchange of spin angular momentum; the direction of this exchange is controlled by the filling factor. An extra alternating current component  $I_2$  can force the phase transition to backtrack to smaller carrier densities, but, as shown in Fig. 7, this current-induced dynamic nuclear polarization occurs only if the frequency  $f_2$  is below 0.01 Hz, whereas the alternating current  $I_1$  used to probe  $R_{SD}$  has a frequency  $f_1$  of 5.36 Hz. This low cut-off frequency is consistent with the previously estimated characteristic response time (a few minutes) of the hyperfine interaction near the ferromagnetic state. □

Received 14 September; accepted 22 November 2001.

1. Prinz, G. A. Magneto-electronics. *Science* **282**, 1660–1663 (1998).
2. Bennett, C. H. & DiVincenzo, D. P. Quantum information and computation. *Nature* **404**, 247–255 (2000).
3. Steane, A. Quantum computing. *Rep. Prog. Phys.* **61**, 117–173 (1998).

4. Ekert, A. & Jozsa, R. Quantum computation and Shor's factoring algorithm. *Rev. Mod. Phys.* **68**, 733–753 (1996).
5. Grover, L. K. Quantum mechanics helps in searching for a needle in a haystack. *Phys. Rev. Lett.* **79**, 325–328 (1997).
6. Cirac, J. I. & Zoller, P. Quantum computations with cold trapped ions. *Phys. Rev. Lett.* **74**, 4091–4094 (1995).
7. Cory, D. G., Fahmy, A. F. & Havel, T. F. Ensemble quantum computing by nuclear magnetic resonance spectroscopy. *Proc. Natl Acad. Sci. USA* **94**, 1634–1639 (1997).
8. Gershenfeld, N. A. & Chuang, I. L. Bulk spin resonance quantum computation. *Science* **275**, 350–356 (1997).
9. Kane, B. E. A silicon based nuclear spin quantum computer. *Nature* **393**, 133–137 (1998).
10. Loss, D. & DiVincenzo, D. P. Quantum computation with quantum dots. *Phys. Rev. A* **57**, 120–126 (1998).
11. Kikkawa, J. M. & Awschalom, D. D. All optical magnetic resonance in semiconductors. *Science* **287**, 473–476 (2000).
12. Kawakami, R. K. *et al.* Ferromagnetic imprinting of nuclear spins in semiconductors. *Science* **294**, 131–134 (2001).
13. Wald, K. W., Kouwenhoven, L. P., McEuen, P. L., van der Vaart, N. C. & Foxon, C. T. Local dynamic nuclear polarisation using quantum point contacts. *Phys. Rev. Lett.* **73**, 1011–1014 (1994).
14. Abragam, A. *The Principles of Nuclear Magnetism* 354–423 (Oxford Univ. Press, Oxford, 1961).
15. Ando, T., Fowler, A. B. & Stern, F. Electronic properties of two-dimensional systems. *Rev. Mod. Phys.* **54**, 437–672 (1982).
16. Eom, J. *et al.* Quantum Hall ferromagnetism in a two-dimensional electron system. *Science* **289**, 2320–2323 (2000).
17. Smet, J. H., Deutschmann, R. A., Wegscheider, W., Abstreiter, G. & von Klitzing, K. Ising ferromagnetism and domain morphology in the fractional quantum Hall regime. *Phys. Rev. Lett.* **86**, 2412–2415 (2001).
18. Côté, R. *et al.* Collective excitations, NMR, and phase transitions in skyrme crystals. *Phys. Rev. Lett.* **78**, 4825–4828 (1997).
19. Das Sarma, S. & Pinczuk, A. (eds) *Perspectives on Quantum Hall Effects* (Wiley, New York, 1996).
20. Girvin, S. M. in *Topological Aspects of Low Dimensional Systems* (eds Comtet, A., Jolicœur, T., Ouvry, S. & David, F.) 53–175 (Springer, Berlin, and EDP Sciences, Les Ulis, 1999).
21. Barrett, S. E., Dabbagh, G., Pfeiffer, L. N., West, K. W. & Tycko, R. Optically pumped NMR evidence for finite-size skyrmions in GaAs quantum wells near Landau level filling  $\nu = 1$ . *Phys. Rev. Lett.* **74**, 5112–5115 (1995).
22. Heinonen, O. (ed.) *Composite Fermions* (World Scientific, Singapore, 1998).
23. von Klitzing, K., Dorda, G. & Pepper, M. New method for high-accuracy determination of the fine-structure constant based on the quantized Hall resistance. *Phys. Rev. Lett.* **45**, 494–497 (1980).
24. Tsui, D. C., Stormer, H. L. & Gossard, A. C. Two-dimensional magnetotransport in the extreme quantum limit. *Phys. Rev. Lett.* **48**, 1559–1562 (1982).
25. Laughlin, R. B. Anomalous quantum Hall effect: an incompressible quantum fluid with fractional charge excitations. *Phys. Rev. Lett.* **50**, 1395–1398 (1983).
26. Jungwirth, T. & MacDonald, A. H. Pseudospin anisotropy classification of quantum Hall ferromagnets. *Phys. Rev. B* **63**, 035305–035314 (2001).
27. Cho, H. *et al.* Hysteresis and spin transitions in the fractional quantum Hall effect. *Phys. Rev. Lett.* **81**, 2522–2525 (1998).
28. Piazza, V. *et al.* First order phase transition in a quantum Hall ferromagnet. *Nature* **402**, 638–641 (1999).
29. De Poortere, E. P., Tutuc, E., Papadakis, S. J. & Shayegan, M. Resistance spikes at transitions between quantum Hall ferromagnets. *Science* **290**, 1546–1549 (2000).
30. Kronmüller, S. *et al.* New type of electron nuclear-spin interaction from resistively detected NMR in the fractional quantum Hall effect regime. *Phys. Rev. Lett.* **82**, 4070–4073 (1999).
31. Hashimoto, K., Muraki, K., Saku, T. & Hirayama, Y. Longitudinal resistance anomaly around the 2/3 filling factor observed in a GaAs/AlGaAs single heterostructure. *Physica B* **298**, 191–194 (2001).
32. Sondhi, S. L., Karlhede, A., Kivelson, S. A. & Rezayi, E. H. Skyrmions and the crossover from the integer to the fractional quantum Hall effect at small Zeeman energies. *Phys. Rev. B* **47**, 16419–16426 (1993).
33. Brey, L., Fertig, H. A., Côté, R. & MacDonald, A. H. Skyrme crystal in a two-dimensional electron gas. *Phys. Rev. Lett.* **75**, 2562–2565 (1995).
34. Tycko, R., Barrett, S. E., Dabbagh, G., Pfeiffer, L. N. & West, K. W. Electronic states in gallium arsenide quantum wells probed by optically pumped NMR. *Science* **268**, 1460–1463 (1995).
35. Bayot, V., Grivei, E., Melinte, S., Santos, M. B. & Shayegan, M. Giant low temperature heat capacity of GaAs quantum wells near Landau level filling  $\nu = 1$ . *Phys. Rev. Lett.* **76**, 4584–4587 (1996).

**Acknowledgements**

We thank A. Stern and L. Brey for discussions, and M. Bichler for technological assistance. This work was supported by the German Ministry of Science and Education (BMBF) and the German Science Foundation (DFG).

**Competing interests statement**

The authors declare that they have no competing financial interests.

Correspondence and requests for materials should be addressed to J.H.S. (e-mail: j.smet@fkf.mpg.de).